Dalton Transactions

The Selectivity of Water-based Pyrophosphate Recognition is Tuned by Metal Substitution in Dimetallic Receptors

Journal:	*Dalton Transactions*
Manuscript ID:	DT-ART-02-2015-000729.R2
Article Type:	Paper
Date Submitted by the Author:	20-May-2015

Complete List of Authors:	McKenzie, Christine; University of Southern Denmark, Department of Physics, Chemistry and Pharmacy Svane, Simon; University of Southern Denmark, Department of Physics, Chemistry and Pharmacy Kjeldsen, Frank; University of Southern Denmark,, Department of Biochemistry and Molecular Biology McKee, Vickie; University of Southern Denmark, Department of Physics, Chemistry and Pharmacy

The Selectivity of Water-based Pyrophosphate Recognition is Tuned by Metal Substitution in Dimetallic Receptors

Simon Svane,[a], [b] Frank Kjeldsen,[b] Vickie McKee,[a] and Christine J. McKenzie[a]*

[a] Department of Physics, Chemistry and Pharmacy, University of Southern Denmark, Campusvej 55 Odense M

[b] Department of Biochemistry and Molecular Biology, University of Southern Denmark, Campusvej 55 Odense M

The three dimetallic compounds $[Ga_2(bpbp)(OH)_2(H_2O)_2](ClO_4)_3$, $[In_2(bpbp)(CH_3CO_2)_2](ClO_4)_3$ and $[Zn_2(bpbp)(HCO_2)_2](ClO_4)$ ($bpbp^-$ = 2,6-bis((N,N'-bis(2-picolyl)amino)methyl)-4-tertbutylphenolate) were evaluated as stable solid state precursors for reactive solution state receptors to use for the recognition of the biologically important anion pyrophosphate in water at neutral pH. Indicator displacement assays using *in situ* generated complex-pyrocatechol violet adducts, $\{M_2(bpbp)(H_xPV)\}^{n+}$ M=Ga^{3+}, In^{3+}, Zn^{2+}, were tested for selectivity in their reactions with a series of common anions: pyrophosphate, phosphate, ATP, arsenate, nitrate, perchlorate, chloride, sulfate, formate, carbonate and acetate. The receptor employing Ga^{3+} showed a slow but visually detectable response (blue to yellow) in the presence of one equivalent of pyrophosphate but no response to any other anion, even when they were present in much higher concentrations. The systems based on In^{3+} or Zn^{2+} show less selectivity in accord with visibly discernable responses to several of the anions. These results demonstrate a facile method for increasing anion selectivity without modification of an organic dinucleating ligand scaffold. The comfortable supramolecular recognition of pyrophosphate by the dimetallic complexes is demonstrated by the single crystal X-ray structure of $[Ga_2(bpbp)(HP_2O_7)](ClO_4)_2$ in which the pyrophosphate is coordinated to the two gallium ions via four of its oxygen atoms.

Introduction

Phosphates, both organic and inorganic, are key substituents for many physiologically important reactions and pathways. The energy requirements for cells are met by hydrolyzing the highly energy rich phosphate anhydride bonds of ATP yielding phosphate and pyrophosphate ($P_2O_7^{4-}$).[1] Phosphate derived from ATP is critical for maintaining crucial cellular signaling pathways and for regulating biochemical reactions.[2, 3] Phosphate is a constituent of the backbone of our genome, well as a building block of cellular membranes and the most widespread post-translational modification occurring in proteins is phosphorylation which affects structure, function and localization.[4] Receptors for the recognition of organic and inorganic phosphates have been reported and the supramolecular interactions which are the basis of the mechanisms of recognition fall into two categories: H-bonding or coordination bonds.[5] Amine-, amide- and urea-based compounds depend on hydrogen-bonding interactions between the phosphate oxygen atoms and proton donors appropriately spatially orientated. A drawback is that these often work best in organic solvents since water will compete for hydrogen bonding sites.[6, 7] Metal complexes exploiting phosphate coordination can function under physiological conditions[8-14] and are hence particularly interesting for the exploitation of selective phosphate recognition in molecular sensors.[15, 16]

The exploitation of either hydrogen bonding or coordination bonds in sensing depends on the host-guest complex showing a distinctly different and easily measurable signal compared to that of the host alone. Fluorescence and colorimetric responses indicating that the desired analyte has been detected are particularly attractive for the implementation of low-tech sensors. The Indicator Displacement Assay (IDA, Figure 1) strategy, pioneered by Anslyn and co-workers,[17, 18] was first employed for detecting citrate using a guandinium-based receptor with carboxyfluorescein as an indicator. This IDA was able to estimate the concentration of citrate in beverages.[17] Falling also within the concept of the IDA strategy, dimetallic zinc complexes of acyclic phenolato- and alkylato-hinged dinucleating ligands 2,6-bis((N,N'-bis(2-picolyl)amino)methyl)-4-methylphenolate ($bpmp^-$)[19-21] and 1,3-bis((N,N'-bis(2-picolyl)amino)methyl)benzene (BBPAB)[22-24] (Figure 2) have been used as receptors for phosphate,[19] ATP[24] and pyrophosphate.[20, 23, 25] In the case of BBPAB a dicopper receptor has also been reported.[22] Dicopper and dinickel complexes based on $bpmp^-$ have been

tested in IDA's against arsenate, phosphate and sulfate where they performed worse than the dizinc analogue.[26] The dizinc complexes of BBPAB showed higher binding constants than complexes of bpmp$^-$ when binding anions. This is likely due to the ligand neutrality and greater flexibility of the dimetallic anion binding site. Conversely greater flexibility may lower the selectivity of BBPAB complexes since anions with different shapes will fit in the less pre-organized binding site. Zinc offers redox stability and, for the most part, forms colorless complexes; both of these features are advantageous when modifying the complexes with chromophores.[27] Developments to enhance selectivity have focused on modifying the organic scaffold of the receptor, or choosing different chromophores as indicators to tune the affinity between receptor and indicator.[20, 21, 28]

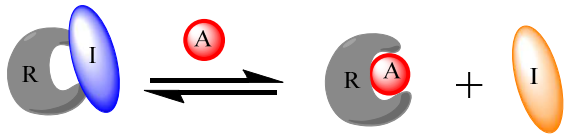

Figure 1. Representation of typical mechanism for IDA signal transduction. R = receptor, I = indicator and A = analyte. The ideal indicator will have significantly different absorption and/or emission intensities and wavelengths between its receptor-bound and free states.

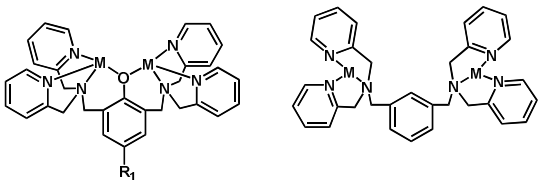

Figure 2. Dimetallic receptor compounds of ligands, bpmp$^-$, bpbp$^-$ and BBPAB.

Less exploited in tuning dimetallic systems for the recognition of anions is the use of different metal ions. The present study examines cationic dimetallic Ga^{3+} or In^{3+}-based anion receptors. Like Zn^{2+} these are d^{10} metal ions, (relatively) redox inactive, and for the main part form colorless compounds. The ionic radii for the Zn^{2+}, Ga^{3+} and In^{3+} ions in 6-coordinated environments are 74, 62 and 80 pm respectively.[29] A homologue of bpmp$^-$, 2,6-bis((N,N'-bis(2-picolyl)amino)methyl)-4-tertbutylphenolate (bpbp$^-$), was employed as the dinucleating ligand scaffold. The initial hypothesis is that the higher charge of the core receptor complex (without auxiliary ligands), $\{M_2(bpbp)\}^{5+}$, M = Ga^{3+}, In^{3+} versus $\{Zn_2(bpbp)\}^{3+}$, will lead to a change in affinities when the complexes are used as receptors for various anions in IDAs.

Experimental

General

All chemicals were purchased from Sigma-Aldrich and used as received. N-(2-hydroxyethyl)piperazine-N'-(2-ethane-sulfonic acid) (HEPES) buffer (pH 7.1), 10 mM, was prepared by dissolving HEPES (0.32 g, 1.34 mmol) and NaHEPES (0.173 g, 0.66 mmol) in 200 ml distilled water obtained from a Millipore-Q system. Nanospray ESI-MS was obtained on an Orbitrap XL mass spectrometer (ThermoFisher, Germany). UV-vis spectra were recorded on an Agilent 8453 UV-vis Spectrophotometer. Elemental analysis was performed at the Chemistry Department II at Copenhagen University, Denmark. Isothermal titration calorimetry (ITC) measurements were carried out on a VP-ITC microcalorimeter (MicroCal Inc.). NMR was performed with an AVANCE III HD (Bruker) with autosampler at 400 MHz. For ^{31}P-NMR 85% H_3PO_4 was used as reference.

Isothermal Titration Calorimetry

The apparent association constant (K_a) for the reaction of pyrophosphate with $[Ga_2(bpbp)(OH)_2(H_2O)_2](ClO_4)_3$ was obtained by titrating 320 µM $Na_4P_2O_7$ (10 mM HEPES solution, pH 7.1) into 1.4095 ml, 17 µM $[Ga_2(bpbp)(OH)_2(H_2O)_2](ClO_4)_3$ (10 mM HEPES solution, pH 7.1) in 30x7 µl portions and measuring the heat change against a reference cell filled with buffer in a VP-ITC MicroCalorimeter (GE Healthcare Life Sciences). All measurements were carried out at 30°C and obtained in triplicate with a reference power of 25 µcal/sec. The K_a, ΔH and ΔS was obtained by fitting the binding heat isotherm (obtained by integrating the heat change) by non-linear regression analysis to the one-site binding model included in the software (Origin) supplied with the instrument.[30] The thermodynamic parameters for the reaction of $[Zn_2(bpbp)(HCO_2)_2](ClO_4)$ with $Na_4P_2O_7$ was obtained in a similar manner except the concentration of the dimetal complex was 25 µM. The thermodynamic parameters for the

reaction of the three dimetallic complexes with Na_2HPO_4 were found by titration of 2.47 mM Na_2HPO_4 into 0.1-0.2 mM solutions (10 mM HEPES, pH 7.1) of each of the dimetal complexes. The titration data and fits are supplied in the supporting information.

UV-vis Spectroscopy

All samples were prepared fresh in 10 mM HEPES buffer (pH 7.1) prior to measurements. All measurements were repeated 3 times. To obtain K_a for the reaction of pyrocatechol violet with $[Zn_2(bpbp)(HCOO)_2](ClO_4)$ and $[Ga_2(bpbp)(OH)_2(H_2O)_2](ClO_4)_3$ stock solutions of 100 μM metal complexes and 200 μM PV were prepared. A series of solutions were mixed with increasing concentrations of metal complex while keeping the indicator constant at 25 μM. The solutions were equilibrated for 20 min before measuring the absorbance at 443 nm. The measured absorbance was corrected for baseline drift by subtracting the absorbance measured at 850 nm (where the receptor:indicator complex does not absorb). The obtained data was fitted by a modified Benesi-Hildebrand[31] plot to yield an apparent K_a.

CAUTION! Although no problems were encountered in the preparation of the perchlorate salts care should be taken when handling such potentially hazardous compounds.

Synthesis

2,6-Bis((N,N'-bis(2-picolyl)amino)methyl)-4-tertbutylphenol (Hbpbp),[32] was synthesized as previously reported.

$[Zn_2(bpbp)(HCOO)_2](ClO_4)\cdot H_2O$. Hbpbp (50 mg, 0.0874 mmol) and sodium formate (20.4 mg, 0.3 mmol) were dissolved in 5 ml MeOH and mixed with $Zn(ClO_4)_2\cdot 6H_2O$ (0.18 mmol) dissolved in 1 ml H_2O. The solution was allowed to evaporate slowly at RT until crystallization of the white product commenced (~2h). Yield: 55.1 mg, 71%, CHN calc.: C: 50.38%; H: 4.78%; N: 9.28%. Found: C: 49.57%; H: 4.52%; N: 9.16%. ESI (MeOH): 100% $[(Zn)_2(bpbp)(HCOO)]^{2+}$ *m/z* 372.0867 (5.1 ppm), 42% $[(Zn)_2(bpbp)(HO)]^{2+}$ *m/z* 358.0892 (5.0 ppm), 24% $[(Zn)_2(bpbp)(HCOO)_2]^{+}$ *m/z* 789.1716 (5.1 ppm), 24% $[(Zn)_2(bpbp)(HCOO)_2]^{+}$ *m/z* 779.1483 (5.1 ppm). ^{1}H NMR (400 MHz, $(CD_3)_2SO$)) δ = 8.74 (d, J = 4 Hz, 2H), 8.56 (s, 2HCOO), 8.22 (d, J = 4 Hz, 2H), 8.04 (t, J = 8 Hz, 2H), 7.64 (d, J = 8 Hz, 2H), 7.54 (t, J = 8 Hz, 2H), 7.37 (t, J = 4 Hz, 2H), 7.12 (t, J = 4 Hz, 2H), 6.61 (s, 2H), 6.46 (d, J = 8 Hz, 2H), 4.38 (d, J = 12 Hz, 2H), 4.10 (d, J = 16 Hz, 2H), 3.80 (d, J = 12 Hz, 2H), 3.56 (d, J = 16 Hz, 2H), 3.36-3.28 (m, 4H), 1.12 (s, 9H) ppm. ^{13}C NMR (100 MHz, $(CD_3)_2SO$) δ = 168.6 (HCOO), 158.1, 154.7, 154.3, 147.2, 145.6, 139.6, 137.9, 137.8, 126.9, 124.4, 124.2, 122.7, 122.2, 121.0, 59.3, 59.1, 57.2, 33.1, 31.5 ppm. IR: ν_a(COO) 1573 cm^{-1}, ν_s(COO) 1444 cm^{-1}

$[Ga_2(bpbp)(OH)_2(H_2O)_2](ClO_4)_3\cdot 4H_2O$. Hbpbp (245 mg, 0.43 mmol) dissolved in 3 ml MeOH was mixed with $Ga(ClO_4)_3\cdot 6H_2O$ (449 mg, 0.94 mmol) dissolved in 2 ml H_2O and the mixture was heated gently for 5 min then left to stand to produce white needles of the product. Yield: 328 mg, 65%. CHN calc.: C: 37.55%; H: 4.64%; N: 7.30%. Found: C: 36.87%; H: 4.00%; N: 7.19%. ESI-MS (MeCN): 90% $[(Ga)_2(bpbp)(O)(OH)]^{2+}$ *m/z* 371.0831 (1.1 ppm), 50% $[(Ga)_2(bpbp)(O)](ClO_4)^{2+}$ *m/z* 412.0560 (3.2 ppm). ^{1}H NMR (400 MHz, D_2O) δ = 8.82 (d, J = 4 Hz, 2H), 8.71 (d, J = 4 Hz, 2H), , 8.26 (t, J = 8 Hz, 2H), 7.83 (d, J = 4 Hz, 2H), 7.74 (t, J = 8 Hz, 4H), 7.47 (t, J = 4 Hz, 2H), 6.97 (s, 2H), 6.76 (d, J = 8 Hz, 2H), 4.83 (d, J = 12 Hz, 2H), 4.59 (d, J = 16 Hz, 2H), 3.36 (d, J = 12 Hz, 2H), 4.03 (d, J = 16 Hz, 2H), 3.80-3.74 (m, 4H), 1.17 (s, 9H) ppm.

$[In_2(bpbp)(CH_3CO_2)_2](ClO_4)_3\cdot 10H_2O$. Hbpbp (50 mg, 0.0874 mmol) was dissolved in 2 ml MeOH and mixed with a 1 ml aqueous solution of $In(ClO_4)_3\cdot 6H_2O$ (91 mg, 0.175 mmol). White needles of the product crystallized on diffusion of ethyl acetate into the solution for several weeks. Yield: 77 mg, 73%. CHN calc.: C: 37.44%; H: 5.11%; N: 6.55%. Found: C: 37.36%; H: 3.51%; N: 6.53%. ESI-MS (H_2O:MeCN): *m/z* 438.0673 $[In_2(bpbp)(O)(CH_3CO_2)]^{2+}$ (calc. 438.0667), *m/z* 417.0614 $[In_2(bpbp)(O)(OH)]^{2+}$ (calc. 417.0614), *m/z* 488.0454 $[In_2(bpbp)(OH)(CH_3CO_2)](ClO_4)^{2+}$ (calc. 488.0449), *m/z* 509.0503 $[In_2(bpbp)(CH_3CO_2)_2](ClO_4)^{2+}$ (calc. 509.0502), *m/z* 468.0778 $[In_2(bpbp)(OH)(CH_3CO_2)_2]^{2+}$ (calc. 468.0773). IR: ν_a(COO) 1576 cm^{-1}, ν_s(COO) 1445 cm^{-1}. ^{1}H NMR (400 MHz, D_2O) δ = 8.97 (bs, 2H), 8.34 (bs, 2H), , 8.24 (bs, 2H), 7.87 (bs, 4H), 7.73 (bs, 2H), 7.27 (bs, 2H), 6.96 (s, 2H), 6.92 (s, 2H), 4.73 (d, J = 16 Hz, 2H), 4.57 (d, J = 16 Hz, 2H), 4.22

(bs, 4H), 4.08 (bs, 2H), 3.65 (s, 2H), 2.03 (s, 6H), 1.11 (s, 9H) ppm. Single crystal X-ray diffraction revealed a complicated double salt formula containing very similar cations: $[In_2(bpbp)(OAc)_2][In_2(bpbp)(OAc)_2(H_2O)]_2(ClO_4)_9 \cdot {}^3/_2H_2O \cdot ½MeOH$. However, mass spectra of crystals obtained from three different syntheses were identical. This, together with the crystal structure indicates a large degree of flexibility for the auxillary acetate and water ligands. An average formulation for the title compound has been used while being aware that water molecules can also be coordinated to the metal.

$[Ga_2(bpbp)(HP_2O_7)](ClO_4)_2 \cdot 3H_2O$.

$[Ga_2(bpbp)(OH)_2(H_2O)_2](ClO_4)_3 \cdot 6H_2O$ (74 mg, 0.062 mmol) was dissolved in 2 ml acetone. $Na_4P_2O_7$ (30 mg, 0.17 mmol) was suspended in 2 ml H_2O and added to the solution of the complex. MeOH (5 ml) was added and 70% $HClO_4$ was added drop-wise until all precipitate had dissolved. The solution was filtered and left open at RT. After several days small white needles suitable for single crystal X-ray analysis were deposited. Yield: 55.2 mg, 77%. ESI-MS: (MeCN): *m/z* 442.0447 $[Ga_2(bpbp)(HP_2O_7)]^{2+}$ (calc. 442.0442), *m/z* 883.0858 $[Ga_2(bpbp)(P_2O_7)]^+$ (calc. 883.0811). CHN calc.: C: 37.96%; H: 4.07%; N: 7.38%. Found: C: 37.59% H: 3.45% N: 7.21 ^{1}H NMR (400 MHz, D_2O) δ = 8.99 (d, J = 4 Hz, 2H), 8.77 (d, J = 4 Hz, 2H), , 8.19 (t, J = 8 Hz, 2H), 7.77 (d, J = 4 Hz, 2H), 7.70 (m, 4H), 7.45 (t, J = 4 Hz, 2H), 6.98 (s, 2H), 6.75 (d, J = 8 Hz, 2H), 4.90 (d, J = 12 Hz, 2H), 4.57 (d, J = 16 Hz, 2H), 4.31 (d, J = 12 Hz, 2H), 4.04 (d, J = 16 Hz, 2H), 3.78 (t, 4H), 1.16 (s, 9H) ppm. ^{31}P-NMR (85% H_3PO_4, D_2O): δ = -7.11 ppm ($Na_4P_2O_7$: δ = -5.95 ppm). IR: ν(P=O) 1120 cm^{-1}, ν(P-O) 1055 cm^{-1}, 1293 cm^{-1}, 1206 cm^{-1}, 576 cm^{-1}.

Indicator Displacement Assay

A typical assay was prepared by dissolving $[Ga_2(bpbp)(OH)_2(H_2O)_2](ClO_4)_3$, $[Zn_2(bpbp)(HCOO)_2](ClO_4)$ or $[In_2(bpbp)(CH_3CO_2)_2](ClO_4)_3$ in 10 mM HEPES buffer, pH 7.1, to form 25 μM solutions of the precursor complexes $[Ga_2(bpbp)(OH)_2(H_2O)_2]^{3+}$, $[Zn_2(bpbp)(HCOO)_2]^+$ or $[In_2(bpbp)(H_2O)(CH_3CO_2)_2]^{3+}$. The indicator pyrocatechol violet (H_4PV), 215 μM in 10 mM HEPES, was then added to the dimetal complex solutions to a final stoichiometry of 1:1 receptor:indicator and left for 20 min to equilibrate. Changes in absorbance caused by addition of different anions at different concentrations were monitored by UV-vis spectroscopy. UV-vis measurements were done 8h after addition of anions.

X-ray Crystallography

Both data sets were collected at 150(2) K on a Bruker Apex II CCD diffractometer using MoK_α radiation (λ = 0.71073Å) and the structures were solved using SHELXT[33] and refined on F^2 using all the reflections.[33] Crystal data, data collection and structure refinement parameters are summarized in Table 1, details specific to each crystal follow.

$[Ga_2(bpbp)(HP_2O_7)](ClO_4)_2 \cdot 3H_2O$. Due to the small size of the crystals, the diffraction data were rather weak. The data were found to be twinned by rotation of 179.9° about reciprocal axis 0 0 1 and were reduced using TWINABS and refined using the resulting HKLF 5 file (BASF 0.261).[34] All the non-hydrogen atoms were refined using anisotropic atomic displacement parameters. Hydrogen atoms bonded to carbon were inserted at calculated positions using a riding model, those bonded to oxygen were inserted with reference to the hydrogen bonding pattern and not refined.

$[In_2(bpbp)(OAc)_2][In_2(bpbp)(OAc)_2(H_2O)]_2(ClO_4)_9 \cdot {}^3/_2H_2O \cdot ½MeOH$. All the non-hydrogen atoms were refined using anisotropic atomic displacement parameters, except for one disordered perchlorate anion, one partial occupancy water molecule and the disordered, partial occupancy methanol molecule. Hydrogen atoms were inserted at calculated positions using a riding model, except for those on the partial-occupancy solvate molecules, which were not included in the model. A general RIGU restraint was applied and Platon SQUEEZE[35] was used to account for some residual diffuse electron density.

Table 1. Details of structure determinations

Complex	$[Ga_2(bpbp)(HP_2O_7)](ClO_4)_2{\cdot}3H_2O$	$[In_2(bpbp)(OAc)_2][In_2(bpbp)(OAc)_2(H_2O)]_2(ClO_4)_9{\cdot}1½H_2O{\cdot}½MeOH$
Chemical formula	$C_{36}H_{46}Cl_2Ga_2N_6O_{19}P_2$	$C_{120.5}H_{144}Cl_9In_6N_{18}O_{55}$
M_r	1139.07	3732.50
Crystal system, space group	Triclinic, $P\bar{1}$	Triclinic, $P\bar{1}$
a, b, c (Å)	10.612(3), 11.395(3), 19.287(6)	10.9425(7), 24.8248(14), 31.3943(19)
α, β, γ (°)	94.225(17), 99.683(18), 104.578(17)	109.057(3), 98.716(4), 91.073(3)
V (Å^3)	2208.6(12)	7946.4(8)
Z	2	2
μ (mm^{-1})	1.50	1.10
Crystal size (mm)	0.16 × 0.11 × 0.05	0.26 × 0.12 × 0.03
No. of measured, independent and observed [I > 2σ(I)] reflections	7541, 7541, 4510	211551, 32479, 19919
R_{int}	N/A(twin)	0.085
R[F^2 > 2σ(F^2)], wR(F^2), S	0.098, 0.253, 1.03	0.054, 0.163, 1.00
$\Delta\rangle_{max}$, $\Delta\rangle_{min}$ (e Å^{-3})	1.54, -0.78	1.92, -1.13

Results and Discussion

Syntheses

Reactive precursor compounds containing the $\{M_2(bpbp)\}^{n+}$ core (M = Zn^{2+} n = 3, Ga^{3+} n = 5 or In^{3+} n = 5), along with various labile auxillary ligands, have been synthesized as described in the experimental section. The precursor complex $[Ga_2(bpbp)(OH)_2(H_2O)_2](ClO_4)_3$ contains aquo and hydroxo ligands which can be exchanged for pyrocatechol violet (H_4PV), the internal base provided by the hydroxo ligands helps drive the reaction. Despite effort, analogous solid state water/hydroxo dizinc, and in the case of diindium, isovalent, complexes could not be isolated. Fortunately a diformate complex, $[Zn_2(bpbp)(HCOO)_2](ClO_4)$, and diacetate complex, $[In_2(bpbp)(CH_3CO_2)_2](ClO_4)_3$ proved to be sufficiently labile in solution for PV adduct formation and the IDA assays described below. The replaceable acetate ligands in $[In_2(bpbp)(CH_3CO_2)_2](ClO_4)_3$ were prepared unusually via ethyl acetate hydrolysis.[36]

The results below show that the digallium complex binds pyrophosphate selectively in an IDA in a 1:1 reaction. We have structurally characterized the adduct as its perchlorate salt, $[Ga_2(bpbp)(HP_2O_7)](ClO_4)_2{\cdot}3H_2O$.

X-ray crystal structures of $[Ga_2(bpbp)(HP_2O_7)](ClO_4)_2{\cdot}3H_2O$ and the diindium precursor complex

The structure of the $[Ga_2(bpbp)(HP_2O_7)]^{2+}$ cation is shown in Figure 3. As expected, the gallium ions are bridged by the phenolate group (Ga1 – Ga2 3.592(2) Å) and each is coordinated facially to three ligand nitrogen donors. The coordination sphere of each metal ion is completed by two oxygen donors of the $HP_2O_7^{3-}$ anion. The anion provides two 3-atom O-P-O bridges linking the metal ions, so the coordination at the metal ions is similar to that in the zinc complex of a related, nitrophenylazo-substituted, ligand.[37] The pyrophosphate anion is a tetradentate donor, leading to complex geometry similar to that in $[M_2(bpbp)(OAc)_2]^{n+}$ ions

with two bridging carboxylates such as cation A of $[In_2(bpbp)(OAc)_2][In_2(bpbp)(OAc)_2(H_2O)]_2(ClO_4)_9 \cdot {}^3/_2H_2O \cdot$ ½MeOH (Fig. 4A) or $[Co_2(bpbp)((PhO)_2PO_2)_2]^{3+}$ [38]. The O-Ga-O bite angles of the chelate ring (94.9(4) and 94.7(4)°) do not impose any sigificant geometric strain on the metal geometry. Selected geometrical parameters for the coordination sphere and bound $HP_2O_7^{3-}$ are given in table 2. The cations are linked into dimers *via* a water molecule which hydrogen bonds to the non-coordinated terminal oxygen atoms O4 and O8 of neighbouring cations.

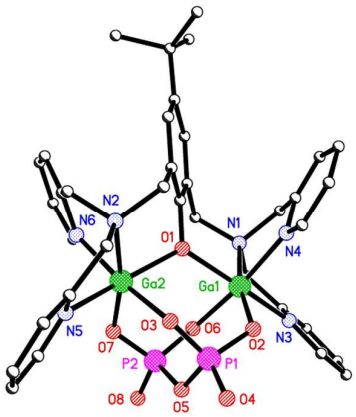

Figure 3. The structure of the cation in $[Ga_2(bpbp)(HP_2O_7)](ClO_4)_2 \cdot 3H_2O$.

The diindium precursor crystallizes as $[In_2(bpbp)(OAc)_2][In_2(bpbp)(OAc)_2(H_2O)]_2(ClO_4)_9 \cdot 1½H_2O \cdot$ ½MeOH, containing three independent cations (A, B and C) in the asymmetric unit along with nine perchlorate anions and several solvate molecules. The three cations are shown in Figure 4, each has different coordination geometry and, although examples of each structural type (two acetates bridging between two metal ions with the same ligand system[39] and bidentate acetate chelating one indium ion[40]) have been reported, it is unusual to find three different arrangements in the same crystal. In the absence of particularly striking intermolecular interactions, this suggests all three are of similar energy. Together they highlight the coordination plasticity of the $\{M_2(bpbp)\}^{n+}$ core. Cation A, $[In_2(bpbp)(OAc)_2]^{3+}$ (Fig. 4A), contains two 6-coordinate indium ions separated by 3.6247(6) Å. Each is coordinated to three nitrogen donors and the bridging phenolate oxygen donor of the $bpbp^-$ ligand; the three N donors adopt the *fac* conformation. The two acetate anions are both bridging but not symmetrical; each makes a normal bond to one indium (*trans* to the tertiary amine) and a somewhat longer interaction with a large C–O–In angle (147.5(4)° at O42A and 149.8(4)º at O51A) to the second (*trans* to a pyridine group). This suggests some geometric strain which may account for the different structures adopted by the other two cations. Cation B (Fig. 4B) has formula $[In_2(bpbp)(OAc)_2(H_2O)]^{3+}$, and the environments of the two metal ions (separation 3.8226 (6) Å) are distinctly different. In1B is 7-coordinate, taking four donors from the $bpbp^-$ ligand (N_3O with the N donors *fac*), it also binds one bidentate acetate anion and the coordination sphere is completed by a second acetate ion which bridges the two metal ions. In2B binds the expected N_3O donors from $bpbp^-$ but with the N donors in the *mer* arrangement; 6-coordination is completed by one oxygen donor from the bridging acetate anion and a water molecule.

Table 2. Selected interatomic distances and angles (Å, º) for $[Ga_2(bpbp)(HP_2O_7)](ClO_4)_2 \cdot 3H_2O$

Ga1—O2	1.914 (9)	Ga2—O7	1.904 (9)
Ga1—O6	1.945 (9)	Ga2—O3	1.952 (10)
Ga1—O1	2.028 (10)	Ga2—O1	2.043 (9)
Ga1—N4	2.038 (11)	Ga2—N6	2.051 (12)
Ga1—N1	2.097 (11)	Ga2—N5	2.081 (11)
Ga1—N3	2.102 (11)	Ga2—N2	2.094 (11)
P1—O4	1.469 (11)	P2—O8	1.480 (10)
P1—O3	1.483 (11)	P2—O6	1.496 (10)
P1—O2	1.555 (10)	P2—O7	1.513 (10)
P1—O5	1.619 (10)	P2—O5	1.620 (11)
Ga1—O1—Ga2	123.9 (5)	P1—O5—P2	121.8 (6)

The C site (Figure 4C) is disordered and was modelled with 50:50 ratio of two cations. The first component is similar to cation B; there is a single bridging acetate group, In1C is facially coordinated and binds a second acetate ion, while In2C is meridonal with a coordinated water molecule. In the second, overlapping component the non-bridging acetate is monodentate rather than bidentate. As a consequence of this difference in the coordination spheres, the indium ion is

disordered over two sites (In1C and In1X) as is one of the pyridine pendant groups. The acetate and phenolate bridges transmit this disorder to the second metal ion which is also disordered over two sites, as are the coordinated water molecule and one pendant pyridine.

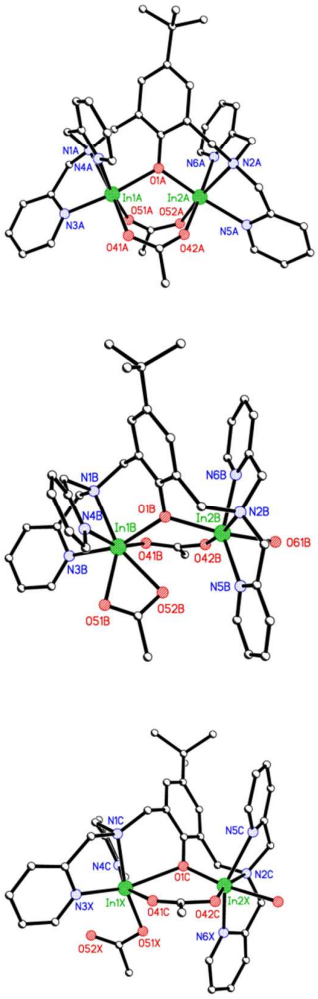

Figure 4. The structures of the cations in $[In_2(bpbp)(OAc)_2][In_2(bpbp)(OAc)_2(H_2O)]_2(ClO_4)_9 \cdot 1½H_2O \cdot ½MeOH$. For the disordered cation C, only the component structurally different from cation B is shown.

Indicator Displacement Assays

The indicator pyrocatechol violet (H_4PV) was chosen for an indicator displacement assay (IDA) since it has been successfully used in topologically similar systems.[19, 20, 26] The precursor complexes were dissolved in 10 mM HEPES buffer to release the ions $[Ga_2(bpbp)(OH)_2(H_2O)_2]^{3+}$, $[Zn_2(bpbp)(HCOO)_2]^{+}$ and $[In_2(bpbp)(CH_3CO_2)_2]^{3+}$ which subsequently reacted with H_4PV to yield 1:1 receptor-indicator adducts $\{Ga_2(bpbp)(H_nPV)\}^{(1+n)+}$, and $\{Zn_2(bpbp)(H_nPV)\}^{(n-1)+}$ as confirmed by Job plots (Fig. 6b and ESI Fig. S1). The reaction could be followed by the clear color change of the yellow H_4PV to deep blue receptor-indicator solutions. It was observed in the Job plot that $[In_2(bpbp)(CH_3CO_2)_2]^{3+}$ does not form a 1:1 complex instead a 3:2 receptor:indicator complex appear to be reached (ESI Fig. S2). Additionally it is clear that at high ratios of indicator new species is likely present in solution since the absorption band moves. This observation combined with suboptimal selectivity in the anion displacement test (Fig. 7c) led to the diindium complex being abandoned as a possible receptor.

Figure 5 illustrates the designed IDA with two possible structures for the generic receptor-indicator adduct as well as the receptor with a bound anionic analyte (here μ_2-O,O′,O′′,O′′′-coordinated pyrophosphate) following displacement of the indicator. The binding mode of pyrophosphate is established by crystallography (above) but no structural data have yet to be reported for any metal complex incorporating pyrocatechol violet. H_4PV has two potential modes for binding to dimetallic complexes; a sulfonic acid group and a catechol, both modes are illustrated in Figure 5.

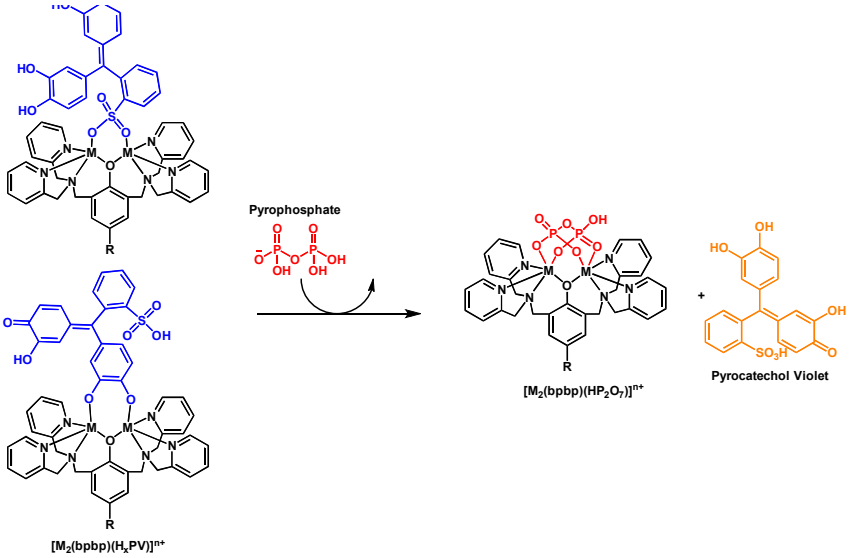

Figure 5. Indicator displacement assay for pyrophosphate with $\{M_2(bpbp)\}^{n+}$ (M = Ga^{3+} n=3 or Zn^{2+} n=1) as receptor and pyrocatechol violet (H_4PV) as indicator. Color code is identical to Figure 1. R = $C(CH_3)_3$.

UV-vis spectroscopy and Anion Sensing

Solutions of pyrocatechol violet in 10 mM HEPES buffer, pH 7.1, are light yellow and change to a deep blue upon addition of solutions containing 1 eq. of $[Ga_2(bpbp)(OH)_2(H_2O)_2]^{3+}$, $[Zn_2(bpbp)(HCOO)_2]^{+}$ or $[In_2(bpbp)(CH_3CO_2)_2]^{3+}$, indicating formation of a receptor-indicator adduct in each case. For example, on addition of the digallium complex to H_4PV, a bathochromic shift in the absorption wavelength from 441 nm (ε = 8319 M^{-1} cm^{-1}) to 603 nm and an extinction coefficient, ε_{603}, of ~11152 M^{-1} cm^{-1} was observed (Figure 6 (a)). A Job plot showed a maximum at 0.5 which indicates a binding stoichiometry of 1:1 receptor:indicator. Similar experiments were carried out for the dizinc and diindium complexes, the absorption maxima and extinction coefficients obtained for all three receptor-indicator complexes are listed in Table 3. $\{Zn_2(bpbp)\}^{3+}$ was found to produce both the largest shift in wavelength and the largest extinction coefficient on binding H_4PV. A Job plot for the titration of $[Zn_2(bpbp)(HCO_2)_2](ClO_4)$ with H_4PV also showed the formation of a 1:1 receptor:indicator complex (ESI, Fig S1). $[In_2(bpbp)(CH_3CO_2)_2](ClO_4)_3$ however, did not show a simple 1:1 stoichiometry (ESI, Fig. S2). The maximum absorbance lies at 0.6 which indicates a 3:2 receptor:indicator complex. To make matters even more complicated at high ratios of pyrocatechol (>2.3 eq.) the absorption band moves towards lower wavelengths (appearing as shoulder in the Job plot) indicating that a new species is likely present in solution.

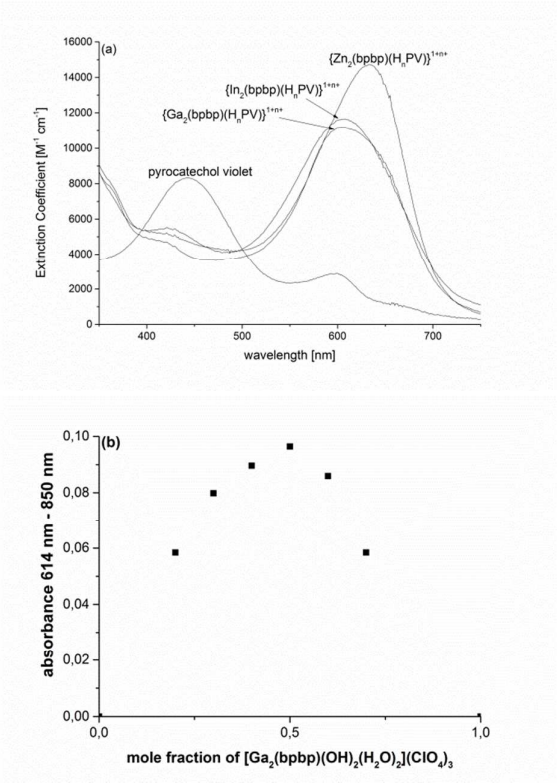

Figure 6. **(a)** UV-vis spectrum of 19 μM H_4PV, $\{Ga_2(bpbp)(H_nPV)\}^{(1+n)+}$, $\{In_2(bpbp)(H_nPV)\}^{(1+n)+}$ and $\{Zn_2(bpbp)(H_nPV)\}^{(n-1)+}$ in 10 mM HEPES buffer, pH 7.2 **(b)** Job plot of $[Ga_2(bpbp)(OH)_2(H_2O)_2](ClO_4)_3$ titrated with increasing amounts of H_4PV in 10 mM HEPES buffer, pH 7.1.

The solubility was too low to get meaningful ^{1}H-NMR spectra which may have yielded more information about the species in solutions of $H_nPV/[In_2(bpbp)(CH_3CO_2)_2](ClO_4)_3$ but.

Table 3. Extinction coefficients and absorption maxima for H_4PV and the $\{M_2(bpbp)(H_nPV)\}^{n+}$ receptor-indicator adducts. The apparent K_a for binding of indicator to receptor was found for those receptors which formed 1:1 complexes ($[Ga_2(bpbp)(OH)_2(H_2O)_2](ClO_4)_3$ and ($[Zn_2(bpbp)(HCO_2)_2](ClO_4)$) by fitting UV-Vis absorption data via a modified Benesi-Hildebrand method.[31]

Compound	A_{max} [nm]	ε_{max} [$M^{-1}cm^{-1}$]	K_a [M^{-1}][a]
H_4PV	441	8319	N/A
$\{Ga_2(bpbp)(H_nPV)\}^{(1+n)+}$	603	11152	$4.28x10^4$
$\{In_2(bpbp)(H_nPV)\}^{(n-1)+}$	608	11653	Not 1:1
$\{Zn_2(bpbp)(H_nPV)\}^{(n-1)+}$	633	14734	$4.45x10^4$

[a] absorption spectra and plots used for the determination of K_a values can be found in supporting information.

The potential of the three receptor complexes for use in IDAs as specific sensors for phosphate, pyrophosphate and ATP was evaluated by adding 11 common anions (as their sodium salts) to different 10 mM HEPES solutions of the receptor-indicator adducts (26-34 μM). Anions which were expected to show low affinity for the receptor complex (mainly the lower charged and weakly-coordinating anions) were added at 100-fold excess. The more highly-charged oxoanions phosphate and arsenate were added at 25- and 50-fold excess respectively. Pyrophosphate and its closest competitor ATP were added at 1 eq.

When $\{Ga_2(bpbp)\}^{5+}$ is chosen as receptor, no immediate color change is observed after adding any anions but after ~8 h at room temperature the sample containing 1 eq. pyrophosphate had changed color from deep blue to a pale green (Figure 7a). At pH 7.1 pyrophosphate exists mainly as mono-protonated (88% $HP_2O_7^{3-}$) and phosphate as a mix of mono- and di-protonated ions (55% H_2PO^{4-} and 45% HPO_4^{2-}) as calculated with HyperQuad[41] software and known pK_a values. The apparent association constant (K_a) for the interaction of these species and the $[Ga_2(bpbp)(OH)_2(H_2O)_2](ClO_4)_3$ receptor was found by isothermal titration calorimetry (ITC) to be $(2.03\pm1.6)x10^7$ M^{-1} with pyrophosphate and $(3.08\pm0.31)x10^6$ M^{-1} with phosphate (Table 4). Phosphate is thus bound ~7 times less strongly than pyrophosphate.

The apparent K_a for binding of PV to the digallium complex was found by UV-vis to be $4.28\pm0.8x10^4$ M^{-1} (table 3). Surprisingly this binding constant is lower than both the binding constants for phosphate and pyrophosphate indicating that the selectivity is governed by another factor.

Table 4. Apparent association constants, K_a, for binding of phosphate and pyrophosphate in 10 mM HEPES buffer, pH 7.1, 30°C.

Solid state precursor for solution state receptor	Anion salt[a]	K_a [M^{-1}]	ΔH [kcal mol^{-1}]	ΔS [cal mol^{-1} K^{-1}]
$[Ga_2(bpbp)(OH)_2(H_2O)_2](ClO_4)_3$	$Na_4P_2O_7$	$(2.03\pm1.6)x10^7$	-4.69±0.3	17.95±2.6
$[Ga_2(bpbp)(OH)_2(H_2O)_2](ClO_4)_3$	Na_2HPO_4	$(3.08\pm0.31)x10^6$	-5.65±0.1	11.03±0.4
$[In_2(bpbp)(CH_3CO_2)_2](ClO_4)_3$	Na_2HPO_4	$(1.22\pm0.27)x10^6$	-4.04±0.2	15.16±1.1
$[Zn_2(bpbp)(HCO_2)_2](ClO_4)$	$Na_4P_2O_7$	$(1.01\pm0.05)x10^7$	-1.64±0.06	-21.93±1.9
$[Zn_2(bpbp)(HCO_2)_2](ClO_4)$	Na_2HPO_4	$(8.60\pm0.66)x10^4$	-4.86±0.06	6.53±0.4

[a]The actual speciation of the anions in solution at pH 7.1 is approximately 4% $H_2P_2O_7^{2-}$/88% $HP_2O_7^{3-}$/8% $P_2O_7^{4-}$ and 55% H_2PO^{4-}/45% HPO_4^{2-} as discussed in the text.

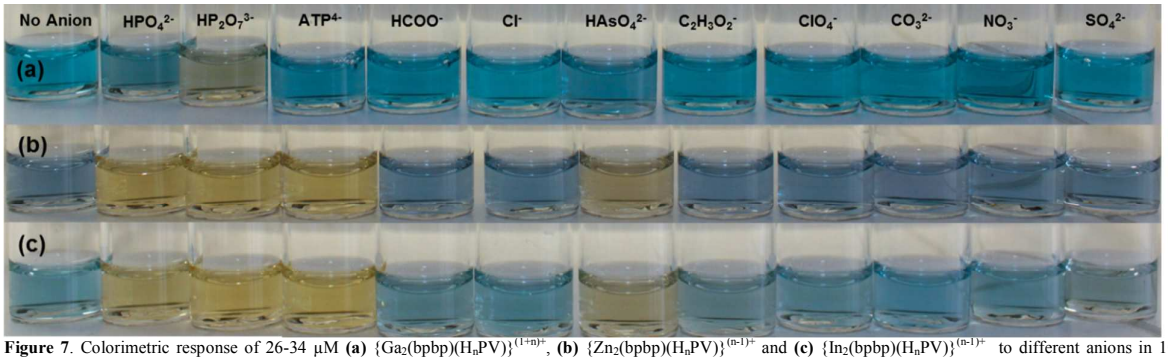

Figure 7. Colorimetric response of 26-34 μM **(a)** $\{Ga_2(bpbp)(H_nPV)\}^{(1+n)+}$, **(b)** $\{Zn_2(bpbp)(H_nPV)\}^{(n-1)+}$ and **(c)** $\{In_2(bpbp)(H_nPV)\}^{(n-1)+}$ to different anions in 10 mM HEPES solution, pH 7.1 after standing in closed vessels for 8h, 25°C. From left to right: no anion, 25 eq. HPO_4^{2-}, 1 eq. $HP_2O_7^{3-}$, 1 eq. ATP^{4-}, 100 eq. $HCOO^-$, 100 eq. Cl^-, 50 eq. $HAsO_4^{2-}$, 100 eq. $CH_3CO_2^-$, 100 eq. ClO_4^-, 100 eq. CO_3^{2-}, 100 eq. NO_3^- and 100 eq. SO_4^{2-}.

Figure 7(b) shows the results using $\{Zn_2(bpbp)\}^{3+}$ as the receptor. This IDA responded significantly faster and after 15 min. no additional color change was observed. However, the selectivity of the receptor-indicator adduct is lower since not only addition of pyrophosphate but also addition of phosphate, ATP and arsenate produced visible color changes from pale blue to yellow. An earlier study utilizing the structurally similar $\{Zn_2(bpmp)\}^{3+}$ as receptor and pyrocatechol violet as indicator found that the system was unable to distinguish between equimolar solutions of pyrophosphate and phosphate as confirmed by the results presented here.[20] Another study found very small differences in the affinity of the $\{Zn_2(bpmp)\}^{3+}$:PV sensor ensemble towards arsenate and phosphate in agreement with the results presented here.[26]

The K_a for the binding of phosphate to $\{Zn_2(bpbp)\}^{3+}$ is ~35 times lower than that found for $\{Ga_2(bpbp)\}^{5+}$ at $(8.60\pm0.66)\times10^4$ M^{-1} (Table 4). The binding of pyrophosphate by $\{Zn_2(bpbp)\}^{3+}$ was, however $(1.01\pm0.05)\times10^7$ M^{-1} (table 4) which is almost equal to that of $\{Ga_2(bpbp)\}^{5+}$. Additionally, the K_a for the binding of PV was 4.45×10^4 (table 3) which is also identical to $\{Ga_2(bpbp)\}^{5+}$. The K_a's measured here for $[Zn_2(bpbp)(HCO_2)_2](ClO_4)$ appear reasonable when compared to those reported for structurally related systems based on the $\{Zn_2(bpmp)\}^{3+}$ core although care should be shown since the constants have been determined in the presence of different counteranions, auxiliary ligands, pH and ionic strengths. The K_a's determined for binding of pyrophosphate differ significantly in magnitude but it is possible that this is caused by differences the lability of the counter anions. Reported values have been collected in table 5 for reference.

Table 5. Apparent association constants, K_a, reported for binding of phosphate, pyrophosphate and PV to the receptor $[Zn_2(bpmp)]^{3+}$.

Source of $[Zn_2(bpmp)]^{3+}$	Anion precursor	K_a [M^{-1}]	ΔH [kcal mol^{-1}]	Buffer/pH	Ref
a	Na_2HPO_4	[c]$(2.08\pm0.5)\times10^4$	-3.68±0.2	100 mM HEPES/7.5	26
b	Na_2HPO_4	[f]$(1.1\pm0.3)\times10^5$	-	5 mM TES, 145 MM NaCl/7.4	21
b	$Na_4P_2O_7$	[f]$(6.7\pm1.8)\times10^5$	-	5 mM TES, 145 mM NaCl/7.4	21
c	Na_2HPO_4	[c]$(1.1\pm0.8)\times10^5$	-7.55±0.1	10 mM HEPES/7.0	19
c	H_4PV	[c]$(5.3\pm0.2)\times10^4$	-11.8±0.1	10 mM HEPES/7.0	19
d	H_4PV	[f]$(3.33)\times10^4$	-	10 mM HEPES/7.4	20

[a] Dissolution of solid $[Zn_2(bpmp)(OAc)_2](BF_4)$. [b-d]Formation *in situ* by the reaction of two equivalents [b] $Zn(NO_3)_2$, [c] $Zn(ClO_4)_2$ or [d] $ZnCl_2$ with bpmpH. [e-f]Measured by [e]ITC, [f]UV-vis.

An IDA using $\{In_2(bpbp)\}^{5+}$ as receptor (Figure 7c) showed color changes within 5-15 min. of adding the anions at rt. However, this receptor showed the same lack of selectivity as $\{Zn_2(bpbp)(H_nPV)\}^{(n-1)+}$ in the colorimetric tests. Addition of pyrophosphate, ATP, phosphate or arsenate all gave rise to a color change from blue to yellow. As revealed by the Job plot the diindium complex does not form a 1:1 receptor:indicator complex with PV which may explain the difference in selectivity. The apparent association constant for the reaction of phosphate with $[In_2(bpbp)(CH_3CO_2)_2]^{3+}$ is $(1.22\pm0.27)x10^6$ M^{-1} (Table 4) which is similar to the result obtained with $[Ga_2(bpbp)(OH)_2(H_2O)_2]^{3+}$ likely reflecting the similar charge of the two complexes.

The enthalpy change was measured for the binding of phosphate and pyrophosphate to the receptor complexes and in all cases the change was found to be negative (table 4) which correlates well with the results obtained for structurally similar dizinc complexes listed in table 5. More interestingly all entropy contributions, however, were found to be positive except for the reaction of pyrophosphate with $[Zn_2(bpbp)(HCO_2)_2](ClO_4)$ which yielded a large unfavorable entropy of -22 cal mol^{-1} K^{-1}.

Perhaps related to the differences in selectivity illustrated above is the fact that during the syntheses of the precursor complexes it was noted that, while $\{In_2(bpbp)\}^{5+}$ and $\{Zn_2(bpbp)\}^{3+}$ readily bound carboxylate auxiliary ligands, $\{Ga_2(bpbp)\}^{5+}$ does not. In support, ESI mass spectra of solutions containing $[Ga_2(bpbp)(OH)_2(H_2O)_2](ClO_4)_3$ and excess benzoate or acetate indicate that $\{Ga_2(bpbp)\}^{5+}$, do not show ions that can be assigned adducts with carboxylate ligands. We speculate that $\{Ga_2(bpbp)\}^{5+}$ is unable to accommodate the bite of a bridging carboxylato groups and this points to subtle differences in the geometries of the dimetallic binding sites. In turn this gives rise to the observed selectivity for specific oxo anions.

In indicator displacement assays it is usually assumed that if the K_a of the analyte is higher than the K_a of the indicator (at equal concentrations) at least partial displacement of the indicator from the receptor should take place if there is no kinetic barrier to overcome. This prediction was shown to be true for a number of indicators (among them PV) with $[Zn_2(bpmp)]^{3+}$ as receptor.[20] This does not, however, appear to be the case in the present study since PV is only displaced from $\{Ga_2(bpbp)\}^{5+}$ by pyrophosphate even when phosphate is added in a 25-fold excess despite the fact that both phosphate and pyrophosphate have a K_a higher than PV. As mentioned the displacement of PV by pyrophosphate takes almost 8h indicating that a kinetic barrier may indeed be present. This reaction time is obviously not optimal for rapid pyrophosphate sensing however the superior selectivity even among structurally related anions should not be ignored. Further development could focus on eliminating the need to replace a dye molecule like in the IDA strategy. For example Hong and co-workers[37] have used the same basic ligand scaffold modified with a fluorescent azophenol moiety (2,6-bis[(bis(2-pyridylmethyl)amino)methyl]-4-nitrophenylazo-4-phenolate). The combination of the $[Ga_2(OH)_2(H_2O)_2]^{4+}$ core with this ligand might be particularly interesting since the direct replacement of the water-derived ligands by pyrophosphate can be anticipated to be fast.[42]

Absorption spectra of solutions of $\{Ga_2(bpbp)(H_nPV)\}^{(1+n)+}$ 8h after addition of anions are shown in Figure 7a). Addition of one eq. of pyrophosphate causes the peak at 622 nm to decrease 66% in intensity and the peak shifted to 580 nm. The peak at 441 nm increases to 72% of the absorbance of unbound H_4PV. These changes translate into a signal easily detected visually as Figure 7a) illustrates. The addition of one eq. ATP to a solution of $\{Ga_2(bpbp)(H_nPV)\}^{(1+n)+}$ also leads to an increase of the peak at 441 nm corresponding to approximately 50% of the response observed for addition of one eq. pyrophosphate. Addition of one eq. of any of the remaining anions causes negligible changes in the absorbance at 622/441 nm.

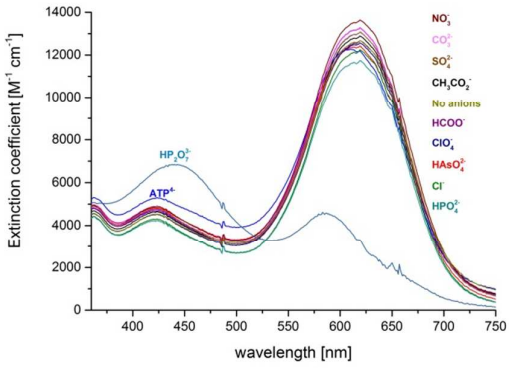

Figure 8. UV-vis spectrum of 25 µM $\{Ga_2(bpbp)(H_nPV)\}^{(1+n)+}$ in 10 mM HEPES, pH 7.1, with different anions after 8h at RT. All anions were present in 25 µM concentrations (1 eq.).

The concentration of ATP^{4-} that causes the displacement of pyrocatechol violet $\{Ga_2(bpbp)(H_nPV)\}^{(1+n)+}$ and gives rise to a visible color change which might interfere with the successful detection of pyrophosphate was identified by increasing amounts of ATP^{4-} added to a solution of 25 µM $\{Ga_2(bpbp)(H_nPV)\}^{(1+n)+}$ (Figure 8). As the concentration of ATP^{4-} was increased the absorption at 622 nm decreased. Interestingly the absorbance at 441 nm did not increase as was seen for one eq. pyrophosphate. Between 10 and 15 eq. of ATP^{4-} were required to cause a visible color change comparable to the change caused by addition of one eq. of pyrophosphate (ESI Fig. S8).

Conclusions

Three labile complexes for generating anion receptor compounds, differing only in the type of metal ions placed in the anion binding site of the receptor $\{Zn^{II}_2(bpbp)\}^{3+}$ and $\{M^{III}_2(bpbp)\}^{5+}$ M = Ga^{3+}, In^{3+} were tested for selectivity towards a series of anions in aqueous solution at pH 7.1: pyrophosphate, phosphate, ATP, arsenate, nitrate, perchlorate, chloride, sulfate, formate, carbonate and acetate. The receptor-indicator adduct $\{Ga_2(bpbp)(H_nPV)\}^{(1+n)+}$ was found to selectively detect pyrophosphate. $\{Zn_2(bpbp)(H_nPV)\}^{(n-1)+}$ was relatively unselective and several anions displaced pyrocatechol violet and gave rise to a visible color change. The diindium receptor did not form 1:1 complexes with PV and it also showed poor selectivity in the displacement assay. The higher charge of $\{Ga_2(bpbp)\}^{5+}$ appears to increase the binding constant for phosphate (relative to that obtained with $\{Zn_2(bpbp)\}^{3+}$) but not the constant for binding pyrophosphate. The relatively long "lag time" from adding pyrophosphate to a solution of $\{Ga_2(bpbp)(H_nPV)\}^{(1+n)+}$ until a color change actually takes place indicates that the digallium receptor/indicator complex is more inert compared to the dizinc and diindium systems in solution and suggests that further refinement is needed to attain a practical receptor-indicator ensemble. The development of sensors and receptors for the selective recognition of biologically important anions is important for example in the field of metabolomics, and for the selective detection of potentially deleterious anions in our environment, e.g. arsenate, nitrates chromates etc. Much work has already been done to increase the sensitivity of dimetallic zinc complexes of ligands similar to the $bpbp^-$ used here e.g. by incorporating fluorophores. Similar strategies might be applied to the development of related Ga^{III}-based systems.

CCDC 1043960 and CCDC 1043961 contain the supplementary crystallographic data for this paper. These data can be obtained free of charge from The Cambridge Crystallographic Data Centre via www.ccdc.cam.ac.uk/data_request/cif.

Acknowledgments

This work was supported by the Danish Council for Independent Research | Natural Sciences (grant 12-124985 to C.McK). Velux Visiting Professorship to V.McK.

References

1. J. K. Heinonen, *Biological Role of Inorganic Pyrophosphate*, Kluwer Academic Publishers, 2001.
2. N. A. Campbell, B. Williamson and R. J. Heyden, *Biology: Exploring Life*, Pearson Prentice Hall, Boston, Massachusetts, 2006.
3. T. Hunter, *Cell*, 2000, 100, 113-127.
4. P. Cohen, *Trends in Biochem. Sci.*, 2000, 25, 596-601.
5. S. Kubik, in *Anion Coordination Chemistry*, Wiley-VCH Verlag GmbH & Co. KGaA, 2011, DOI: 10.1002/9783527639502.ch7, ch. 7, pp. 363-464.
6. K. Niikura, A. Metzger and E. V. Anslyn, *J. Am. Chem. Soc.*, 1998, 120, 8533-8534.
7. D. H. Vance and A. W. Czarnik, *J. Am. Chem. Soc.*, 1994, 116, 9397-9398.
8. J. Gao, T. Riis-Johannessen, R. Scopelliti, X. H. Qian and K. Severin, *Dalton Trans.*, 2010, 39, 7114-7118.
9. S. Mizukami, T. Nagano, Y. Urano, A. Odani and K. Kikuchi, *J. Am. Chem. Soc.*, 2002, 124, 3920-3925.
10. M. Hosseini, M. R. Ganjali, M. Tavakoli, P. Norouzi, F. Faridbod, H. Goldooz and A. Badiei, *J. Fluoresc.*, 2011, 21, 1509-1513.

11. M. R. Ganjali, M. Hosseini, F. Aboufazeli, F. Faridbod, H. Goldooz and A. R. Badiei, *Luminescence*, 2012, 27, 20-23.
12. J. F. Zhang, S. Kim, J. H. Han, S. J. Lee, T. Pradhan, Q. Y. Cao, S. J. Lee, C. Kang and J. S. Kim, *Org. Lett.*, 2011, 13, 5294-5297.
13. X. J. Zhao, L. He and C. Z. Huang, *Talanta*, 2012, 101, 59-63.
14. M. Strianese, S. Milione, A. Maranzana, A. Grassi and C. Pellecchia, *Chem. Comm.*, 2012, 48, 11419-11421.
15. V. Amendola and L. Fabbrizzi, *Chem. Comm.*, 2009, DOI: Doi 10.1039/B808264m, 513-531.
16. K. Suntharalingam, A. J. P. White and R. Vilar, *Inorg. Chem.*, 2010, 49, 8371-8380.
17. A. Metzger and E. V. Anslyn, *Angew. Chem. Int. Ed.*, 1998, 37, 649-652.
18. A. E. Hargrove, S. Nieto, T. Zhang, J. L. Sessler and E. V. Anslyn, *Chem. Rev.*, 2011, 111, 6603-6782.
19. M. S. Han and D. H. Kim, *Angew. Chem. Int. Ed.*, 2002, 41, 3809-3811.
20. B. P. Morgan, S. He and R. C. Smith, *Inorg. Chem.*, 2007, 46, 9262-9266.
21. R. G. Hanshaw, S. M. Hilkert, J. Hua and B. D. Smith, *Tetrahedron Lett.*, 2004, 45, 8721-8724.
22. S. Y. Kim and J.-I. Hong, *Tetrahedron Lett.*, 2009, 50, 1951-1953.
23. S. Kim, M. S. Eom, S. K. Kim, S. H. Seo and M. S. Han, *Chem. Comm.*, 2013, 49, 152-154.
24. M. S. Han and D. H. Yim, *Bull. Korean Chem. Soc.*, 2004, 25, 1151-1155.
25. H. J. Kim, J. H. Lee and J. I. Hong, *Tetrahedron Lett.*, 2011, 52, 4944-4946.
26. C. D. Moffat, D. J. Weiss, A. Shivalingam, A. J. White, P. Salaun and R. Vilar, *Chemistry*, 2014, 20, 17168-17177.
27. H. T. Ngo, X. Liu and K. A. Jolliffe, *Chem. Soc. Rev.*, 2012, 41, 4928-4965.
28. X. Liu, H. T. Ngo, Z. Ge, S. J. Butler and K. A. Jolliffe, *Chem. Sci.*, 2013, 4, 1680-1686.
29. R. D. Shannon, *Acta Cryst.*, 1976, 32, 751-767.
30. I. Jelesarov and H. R. Bosshard, *J. Mol. Recog.*, 1999, 12, 3-18.
31. P. R. Hammond, *J. Chem. Soc.*, 1964, 479-484.
32. M. Ghiladi, K. B. Jensen, J. Jiang, C. J. McKenzie, S. Moerup, I. Soetofte and J. Ulstrup, *Dalton Trans.*, 1999, 2675-2681.
33. G. M. Sheldrick, *Acta Cryst.*, 2015, C71, 3-8.
34. G. M. Sheldrick, Bruker AXS Inc., Madison, Wisconsin, USA, 2012-1 edn., 2012.
35. P. van der Sluis and A. L. Spek, *Acta Cryst. A* 1990, 46, 194-201.
36. M. Ghiladi, C. J. McKenzie, A. Meier, A. K. Powell, J. Ulstrup and S. Wocadlo, *Dalton Trans.*, 1997, 0, 4011-4018.
37. D. H. Lee, J. H. Im, S. U. Son, Y. K. Chung and J. I. Hong, *J. Am. Chem. Soc.*, 2003, 125, 7752-7753.
38. F. B. Johansson, A. D. Bond, U. G. Nielsen, B. Moubaraki, K. S. Murray, K. J. Berry, J. A. Larrabee and C. J. McKenzie, *Inorg. Chem.*, 2008, 47, 5079-5092.
39. R. K. Seidler-Egdal, F. B. Johansson, S. Veltze, E. M. Skou, A. D. Bond and C. J. McKenzie, *Dalton Trans.*, 2011, 40, 3336-3345.
40. H. Preut and F. Huber, *Z. Anorg. Allg. Chem.*, 1979, 450, 120-130.
41. A. L., G. P. and I. A., *Coord. Chem. Rev.*, 1999, 84, 311-318.
42. S. Svane, F. Kryuchkov, A. Lennartson, C. J. McKenzie and F. Kjeldsen, *Angew. Chem. Int. Ed.*, 2012, 51, 3216-3219.